UCRL-JC-129771
PREPRINT

Implementation of Smoothing by Spectral Dispersion on Beamlet and NIF

J. E. Rothenberg
J. M. Auerbach
B. D. Moran
J. E. Murray
T. L. Weiland
P. J. Wegner

This paper was prepared for submittal to the
Third Annual International Conference on
Solid State Lasers for Application (SSLA)
to Inertial Confinement Fusion (ICF)
Monterey, California
June 7-12, 1998

August 25, 1998

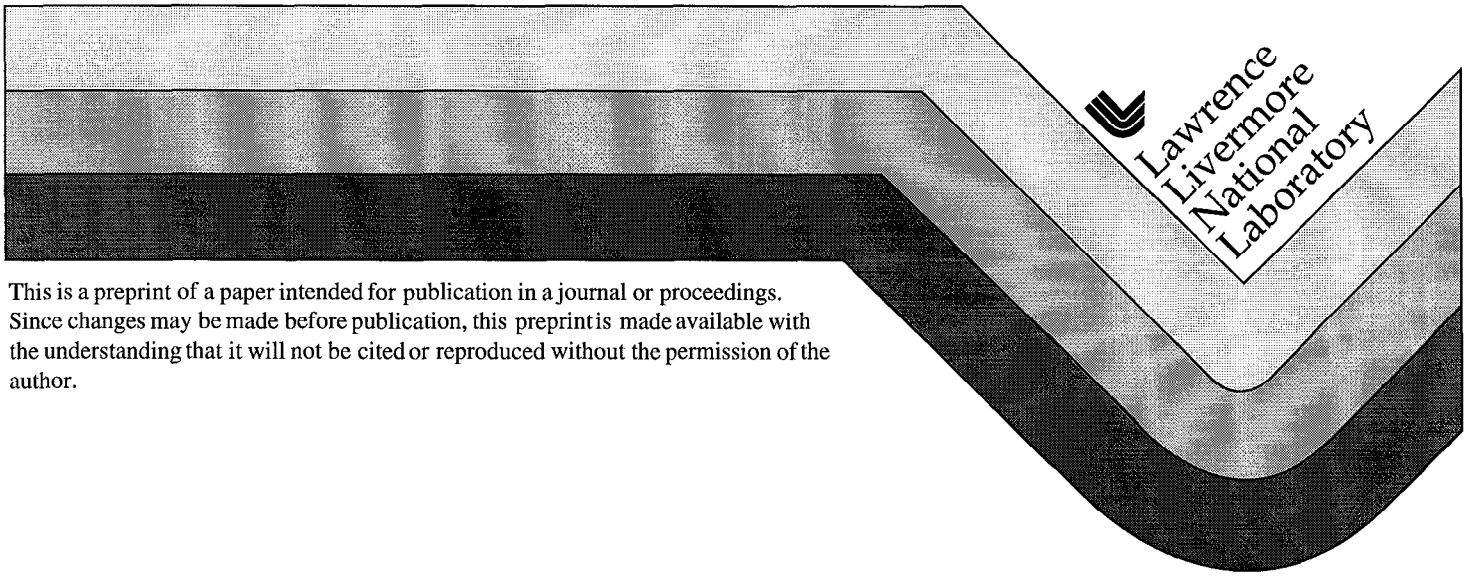

Implementation of Smoothing by Spectral Dispersion on Beamlet and NIF

Joshua E. Rothenberg, Jerome M. Auerbach, Bryan D. Moran,
James E. Murray, Timothy L. Weiland, and Paul J. Wegner

Lawrence Livermore National Laboratory, L-439,P. O. Box 808, Livermore, CA 94551
Telephone: (510) 423-8613 , FAX: (510) 422-5537 , Email: JR1 @ LLNL.GOV

ABSTRACT

The performance of the Beamlet laser with one dimensional smoothing by spectral dispersion (1D SSD) implemented is investigated. Measurements of the near field beam quality, nonlinear breakup, and transmission through spatial filter pinholes show a modest effect only at large SSD divergence. No measurable effect was found at the divergence level planned for indirect drive ignition experiments. The efficiency of conversion to the third harmonic was also measured with SSD present and found to be somewhat larger than expected from an ideal plane wave model.

Keywords: Beam smoothing, smoothing by spectral dispersion, laser plasma instabilities, inertial confinement fusion.

1. INTRODUCTION

Optimal performance of the inertial confinement fusion (ICF) target requires that the driver laser beam be spatially conditioned such that the illumination on target is sufficiently uniform. For indirect drive the enhancement of laser plasma instabilities by illumination nonuniformity underlies the requirement to smooth the target illumination. For direct drive, a much smoother beam is required because the illumination nonuniformity is directly imprinted onto the target surface and is subsequently amplified by hydrodynamic instabilities. A number of approaches have been suggested to achieve the desired level of uniformity for ICF.[1-8] All these approaches make use of target illumination which is comprised of a time varying speckle pattern. Over a characteristic integration time set by target physics, the addition of statistically independent speckle patterns blurs out the instantaneous spatial variations of intensity on the target. The SSD method[4] is particularly well suited to ICF with glass lasers because the pure phase modulation used preserves the near field beam quality, and thereby allows for efficient extraction of energy from the amplifiers. For a modest uniformity requirement (indirect drive, RMS 15 - 25 %) it is thought that the 1D SSD method is sufficient, and for a more uniform beam (direct drive, RMS < 10%) 2D SSD is required.[7] A schematic of the 1D SSD technique is shown in Fig. 1. In the usual implementation, pure sinusoidal phase modulation (FM) is imposed on the low power beam in the laser front end. A diffraction grating or other dispersive element then induces angular divergence on the beam. Each FM sideband is shifted off axis in proportion to its frequency shift, and thus the 1D SSD beam would focus to a series of shifted spots in a line in the far field (hence, 1D SSD). With the presence of a random phase plate,[2] this series of far field focal spots becomes a series of shifted speckle patterns. To obtain

optimal smoothing these speckle patterns must be shifted by at least the half width of a speckle, which, expressed as a far field angle is λ / D, where D is the final beam width. This requirement is referred to as "critical dispersion", and is equivalent to requiring the grating to impose a temporal skew across the beam equal to the period of the phase modulator. For Beamlet or NIF, the minimum angular shift between sidebands is λ / D ~3 μrad, and if N sidebands are imposed by the modulator, the required beam divergence in the main cavity will be ~3· N μrad. Thus, to minimize the divergence at critical dispersion for a given bandwidth one must minimize the number of sidebands, and hence maximize the frequency of modulation. The increased divergence provides an essential limitation for 1D SSD, i.e. increased clipping from the spatial filter pinholes, which leads to increased near field modulation and therefore reduced amplifier extraction. Based on our current understanding of the target requirements, it is anticipated that the 1D SSD divergence required for indirect drive is ~ ±7.5 μrad, and for direct drive 2D SSD is required with as much as ±25 μrad. In this paper we describe experiments and numerical simulations which address the issue of performance of Beamlet with 1D SSD.

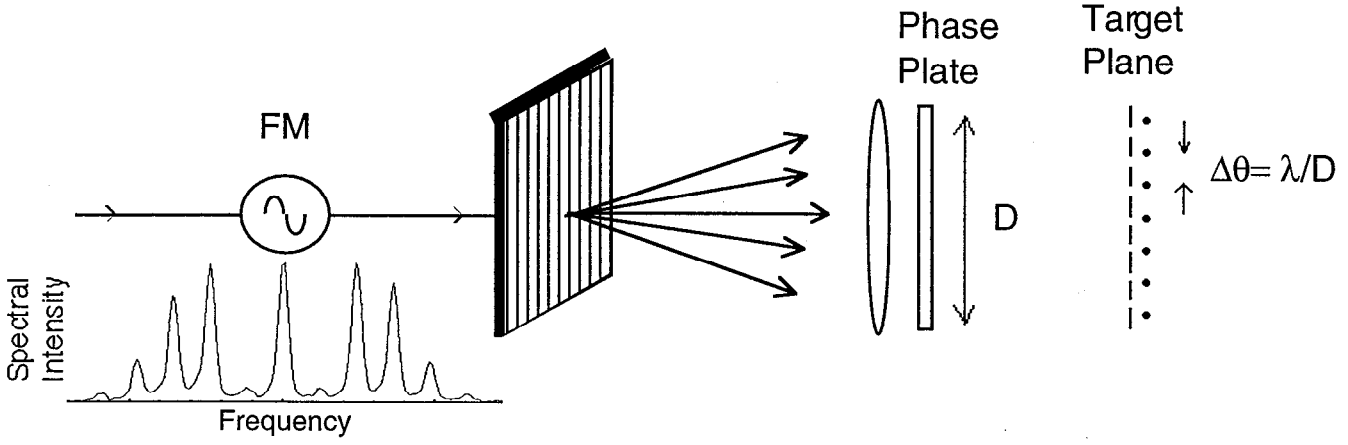

Figure 1: Schematic of the arrangement used for the 1D SSD method. Without a phase plate, each sideband of the modulator would focus to a spot shifted by a minimum angle (λ / D). The phase plate then generates a series of speckle patterns, each shifted by this angle.

2. EXPERIMENTAL ARRANGEMENT

Figure 2 shows the modifications which were made to Beamlet to allow for the implementation of SSD. An integrated optic phase modulator in the master oscillator room was used to impose varying amounts of FM on the beam. After amplification by the regenerative amplifier and spatial shaping, the beam is usually directed by two turning mirrors towards the four pass preamplifier (path shown in bold). Instead, one of these mirrors (now on a kinematic mount) is removed and the beam enters the SSD apparatus. The grating is oriented for exact Littrow diffraction, which allows the simple interchange of gratings of varied dispersion. The diffracted beam is picked off by a 50% beam splitter and directed back into the four pass

preamplifier. This arrangement although lossy (the throughput is ~20%), is convenient in that it provides a simple means of maintaining the grating in the exact Littrow configuration.

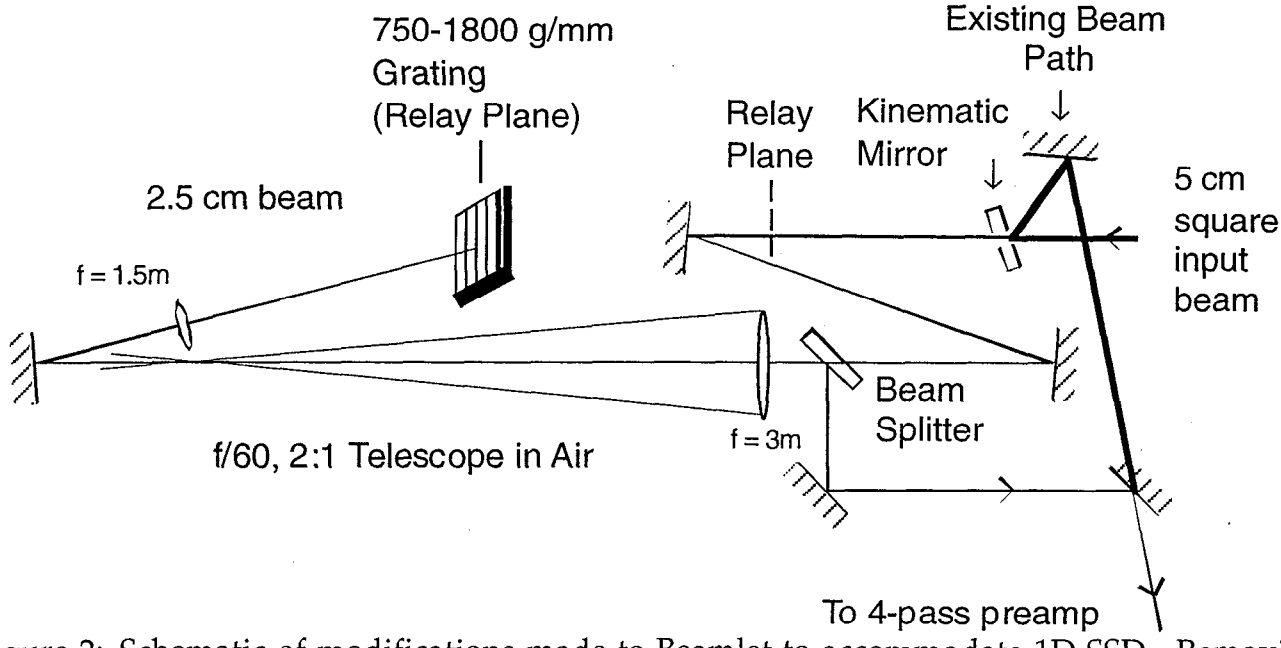

Figure 2: Schematic of modifications made to Beamlet to accommodate 1D SSD. Removing the kinematic mirror allows the beam to traverse the SSD section before going to the four pass preamplifier.

To minimize the SSD divergence required for indirect drive, a new high frequency modulator was developed. This modulator can provide up to 5 Å of bandwidth in the IR and was operated at 17 GHz modulation frequency. Figure 3 shows a spectral scan of the modulated output obtained with a high resolution Fabry-Perot spectrometer. As indicated, the central sideband is suppressed for this modulation depth (2.4). The two sidebands on each side are separated by the 17 GHz modulation frequency; a third sideband on each side is outside of the range of the Fabry-Perot.

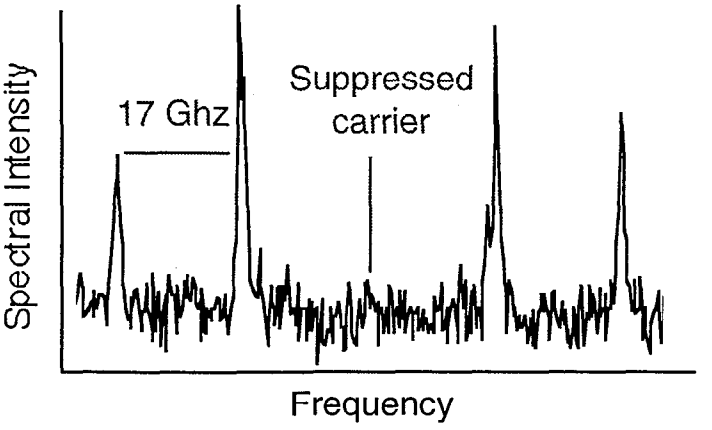

Figure 3: Spectrum of FM 1ω beam measured with a Fabry-Perot. The modulation frequency is 17 GHz and the depth is 2.4, for a total bandwidth of ~ 3 Å.

The effect of the SSD grating on the far-field intensity distribution at the Beamlet 1ω output is shown in Fig. 4. In Fig. 4 (a), 5 Å bandwidth generated by the 17 GHz modulator is critically dispersed, and in 4 (b) the dispersion is increased to three times critical. At the larger dispersion each sideband is clearly separated, and one can see that a divergence greater than 50 μrad can be generated.

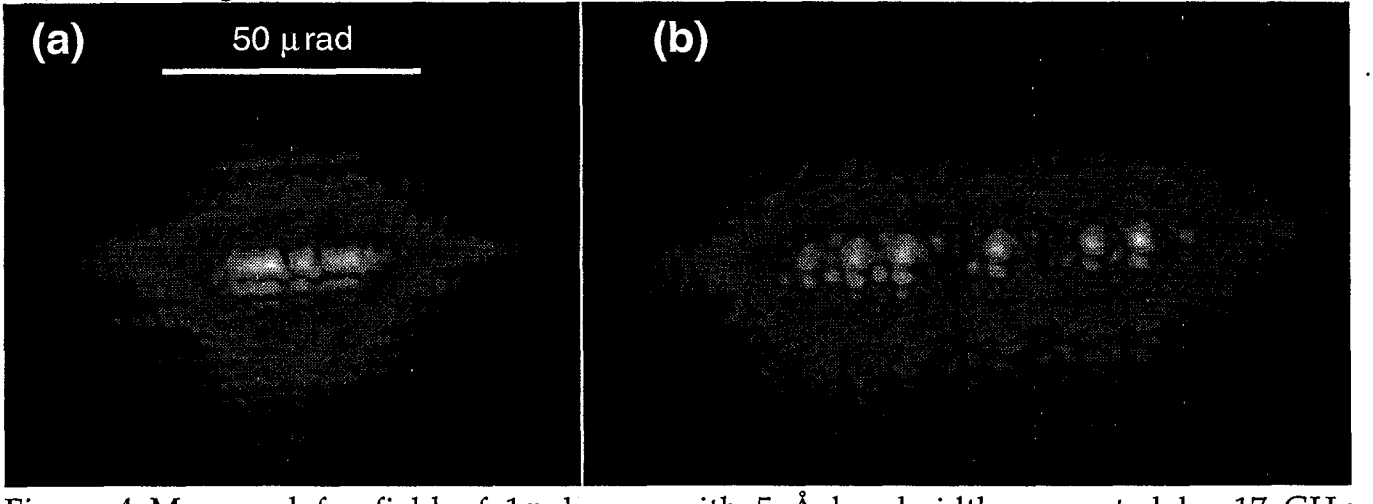

Figure 4: Measured far field of 1ω beam, with 5 Å bandwidth generated by 17 GHz modulator. (a) critical dispersion and (b) three times critical dispersion.

2. PINHOLE CLOSURE WITH SSD

The problem of plasma blowoff occluding the beam transmitted through spatial filter pinholes has been investigated without the presence of SSD, and a new cone-shaped pinhole design has been found to be beneficial in extending the spatial filter transparency for the full length of ICF ignition pulse shapes.[9] The extent to which the plasma blowoff interferes with the transmitted beam is strongly dependent upon the intensity loading on the pinhole edges, and thus one

would expect some degradation of transmission as SSD divergence is imposed on the beam. Here, a ±100 μrad tantalum cone pinhole was used in the transport spatial filter to investigate the effect of SSD on pinhole closure with 20 ns square pulses. Closure of the pinhole is determined by measurement of the 1ω output near field intensity contrast with a streak camera. As the pinhole nears closure there is a dramatic increase in the contrast. The effect of SSD with ±7.5 μrad divergence on closure is shown in the streak data of Fig 5 (a), which compares nearly equal energy pulses with and without SSD present. One sees that for these shots the pinhole stays open slightly longer with SSD present. Although the experimental uncertainties do not allow us to conclude that SSD at this divergence level is actually beneficial for the problem of pinhole closure, one can conclude that it does not significantly accelerate closure. However, at larger levels of SSD divergence one does observe a significant decrease in the pulse energy required to cause closure of this cone tantalum pinhole during the 20 ns pulse length, as shown in Fig 5 (b).

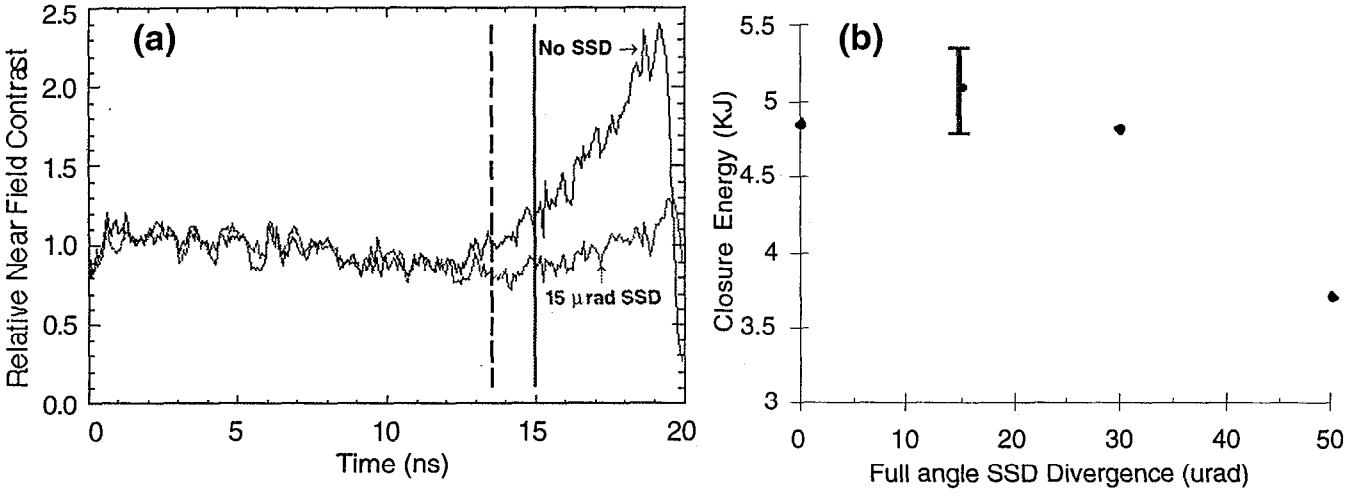

Figure 5: Measured behavior of the closure of ±100 μrad tantalum pinhole in the presence of SSD. (a) Contrast at the 1ω output of a 20 ns square pulse as measured with a streak camera with and without SSD of ±7.5 μrad (i.e. 15 μrad full angle) divergence. (b) Energy required to cause closure during the 20 ns pulse versus the amount of (full angle) SSD divergence.

3. EFFECT OF SSD AND B-INTEGRAL ON NEAR FIELD BEAM QUALITY

Numerical simulations of beam propagation for Beamlet and NIF show that the contrast of the near field intensity is degraded by nonlinear effects (B-integral). One sees in the PROP92 calculations of Fig. 6, that these effects are most severe when the spatial filter pinhole size is increased, since the ripples from larger angle rays grow more rapidly, and that the presence of SSD divergence also degrades the contrast. As a result one is concerned that SSD will cause some decrease in the margin against beam breakup.

This effect was investigated using 0.5 ns pulse with the booster amplifiers unpumped to obtain large ΔB integral between the last cavity pinhole (±167 μrad) and the 1ω output. In addition to the near field fine structure resulting from the nonlinearity, the intensity also varies slowly

across the beam aperture. Therefore to assess the dependence of contrast on ΔB, the beam was divided into 36 5x5 cm patches and the contrast was calculated in each patch and plotted versus the calculated average ΔB integral corresponding to the average intensity in that patch. These measurements were made both without SSD and with SSD of increasing divergence. The results are shown in Fig. 7, where the plusses correspond data taken without SSD (but with bandwidth) present, and the square data points correspond to data taken with the indicated level of SSD.

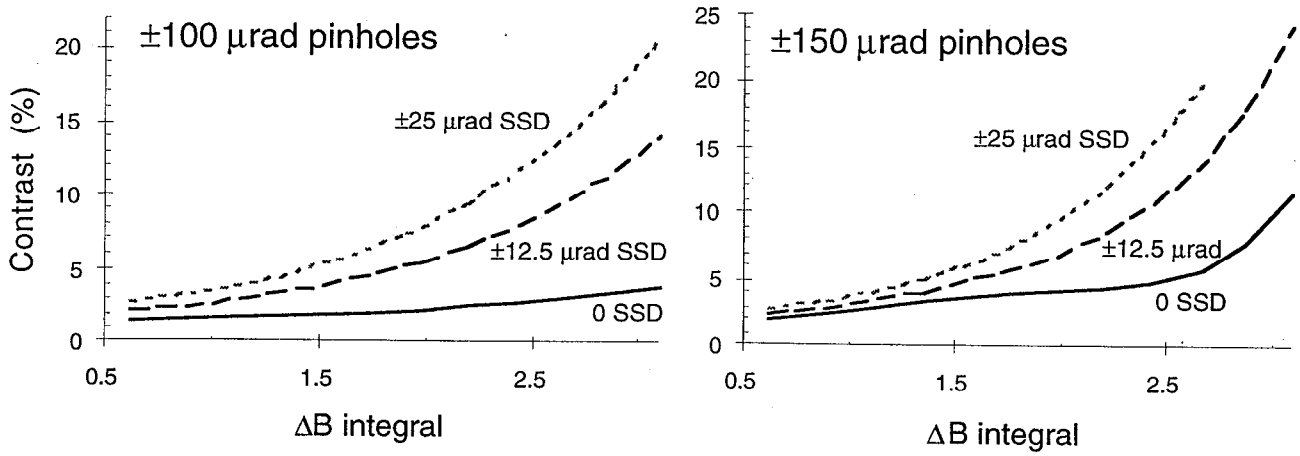

Figure 6: Numerical simulations using PROP92 of the Beamlet output 1ω near field intensity contrast as a function of ΔB integral for 1 ns pulses, for the indicated pinhole sizes and amount of SSD divergence.

One sees that at ±15 μrad SSD no significant degradation is observed compared to the data taken without SSD. However, at ±25 μrad SSD one does observe some degradation at the largest values of ΔB . Although the number of data points at higher contrast is limited, it appears that for ±25 μrad SSD the beam breakup is occurring at ΔB smaller by ~ 0.2 (~ 10% reduction). It is noteworthy, however, that within the variations of these measurements there is no significant beam degradation observed at ±25 μrad SSD for ΔB <1.9, when compared to the data obtained without SSD present.

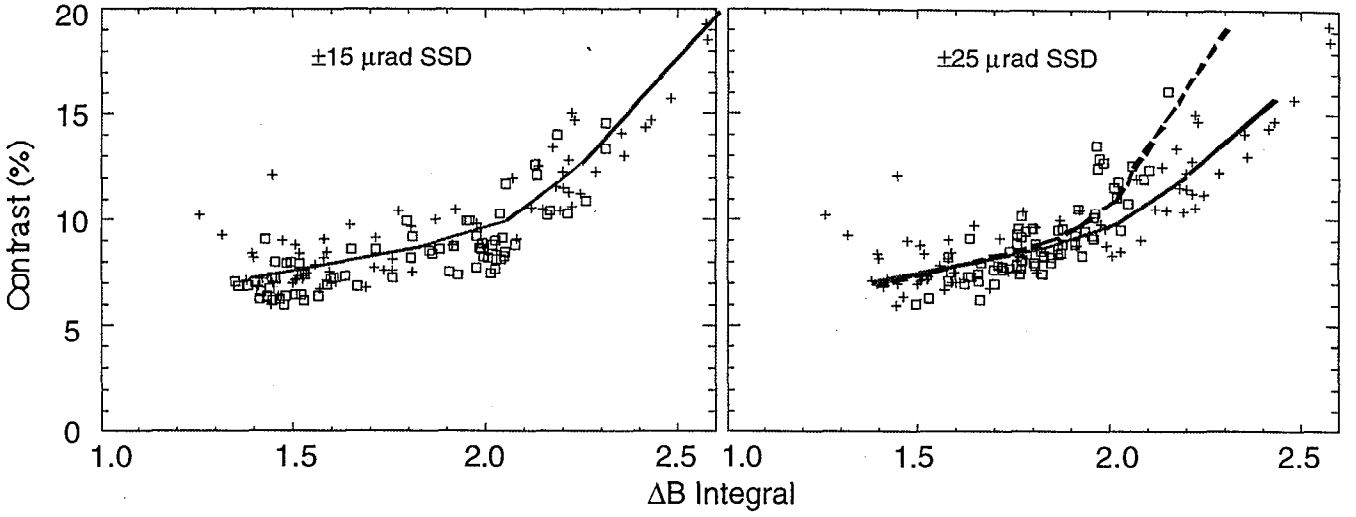

Figure 7: Measured contrast in 5x5 cm patches of the Beamlet 1ω output near field beam, with the indicated amount of SSD divergence (squares, dashed line) and without SSD (plusses, solid curve). No significant degradation is found for ±15 μrad SSD, but there is some effect at ±25 μrad. The curves are only guides for the eye. ΔB is calculated for propagation from the last ±167 μrad cavity pinhole to the 1ω output.

4. THIRD HARMONIC FREQUENCY CONVERSION WITH SSD

The requirement for SSD bandwidth is thought to be ~ 3 Å in the IR for indirect drive and ~ 5 Å or greater for direct drive. Simulations[11] and previous measurements[8] indicate that the conversion efficiency will decrease significantly, especially at larger bandwidths. The conversion configuration of Beamlet (11 mm type I KDP doubler and 9.5 mm type II KD*P tripler) is quite similar to the 11/9 mm baseline design for NIF, and thus should give a good indication of the expected performance. Extensive measurements of the third harmonic energy conversion on Beamlet have been performed in the absence of SSD using 1.5 ns pulses and carefully calibrated harmonic energy detectors (accuracy better than 1%).[10] Using these calibrated detectors, the third harmonic energy conversion performance with SSD present was measured with 1.5 ns input pulses of intensity ~3.0 GW/cm^2 for a limited number of bandwidth and dispersion configurations.

These measurements are shown in Fig. 8, along with simulations of ideal plane wave conversion. The dark solid curve is the result of the ideal plane wave calculation of conversion efficiency versus bandwidth without SSD dispersion, and then the efficiencies are linearly scaled to match the experimental result at 1 Å bandwidth (triangle, measured at 73.3%, whereas the ideal plane wave calculation yields 83%). A number of effects have been found to contribute to this reduction (e.g. temporal and transverse profiles, crystal uniformity, and degraded anti-reflection coatings), but are not considered in the initial calculations presented here. The dotted and dashed curves are calculations of efficiency including the effect of SSD with critical and three times critical dispersion, respectively. In these calculations the grating dispersion was assumed to be oriented such that the angular dispersion of the bandwidth

partially compensates for the phase mismatch in the tripler, and thus the SSD dispersion modestly increases the conversion efficiency.

The conversion efficiency with 3 and 5 Å IR bandwidth, generated by the 17 GHz modulator, was measured with SSD of critical dispersion and is shown by triangles connected by a light solid line. The SSD grating for these two data points was oriented to assist phase matching in the tripler. A measurement taken at 3 Å with the grating orientation reversed (cross) shows that the efficiency is reduced from ~ 69 to 67%, larger than the 0.7% reduction the calculations indicate, but close to the accuracy of the measurement.

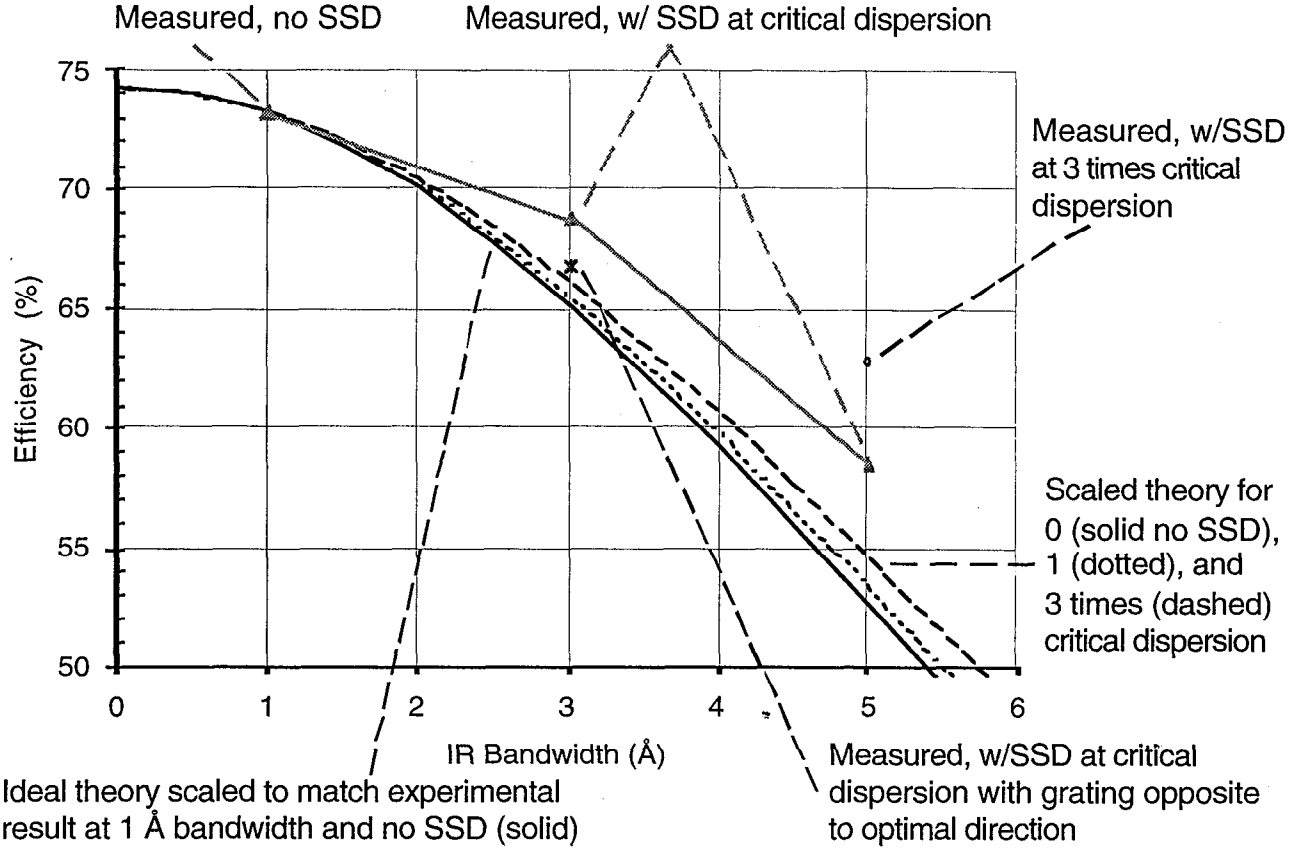

Figure 8: Calculated and measured efficiency of third harmonic energy conversion with 1.5 ns, ~ 3.0 GW/cm^2 pulses. Dark solid curve is the calculated efficiency without SSD using an ideal plane wave model which has been linearly scaled to match the measurement at 1 Å bandwidth and no SSD (triangle). Dotted and dashed curves are calculations with SSD of critical and three times critical dispersion, respectively, and the grating oriented to assist phase matching in the tripler. Triangles at 3 and 5 Å are measurements made with critical dispersion and the grating oriented to assist phase matching. Cross at 3 Å is a measurement with critical dispersion, but opposite grating orientation. Circle at 5 Å is a measurement with three times critical dispersion and grating oriented to assist phase matching.

A more significant effect was found at 5 Å bandwidth, where the conversion was measured to increase from 58.6 to 62.9%, when the dispersion was increased from critical to three times critical (circle), and the grating was oriented to assist phase matching. This 4.3% increase is significantly larger than the 1.3% value the scaled ideal plane wave theory predicts. Note that the linearly scaled ideal plane wave model indicates a lower efficiency than all the data taken at 3 and 5 Å, and thus indicates a significant effect is absent from the model and is bandwidth sensitive. An initial investigation of this issue indicates that the variation of pointing of the optic axis throughout the volume of the tripler may be partially responsible for both a reduction in conversion at low bandwidth and the relative improvement at larger bandwidth. That is, this variation, in effect, would both broaden and reduce the peak of the phase matching curve in the tripler.

5. CONCLUSIONS

Measurements of the performance of Beamlet demonstrate a modest sensitivity to the implementation of 1D SSD. At the baseline level of SSD for indirect drive (±7.5 μrad), neither a significant effect on pinhole closure nor nonlinear (B-integral induced) beam breakup was observed. At the ±25 μrad level required for direct drive there is a ~ 10% reduction (2.2 → 2.0) in the ΔB integral required to initiate beam breakup. Pinhole closure was also observed to be accelerated with ±25 μrad SSD, indicating that a small (~ ±10 μrad) increase in pinhole size (relative to indirect drive) might be required. Finally, it was found that frequency conversion with SSD bandwidth was somewhat better than calculated with a simple linearly scaled plane wave model, and that the presence of SSD dispersion was more beneficial than anticipated when the grating was properly oriented. The measured relative reduction in efficiency compared to the configuration of 1 Å bandwidth without SSD was 6% (73.3 → 68.9%) for 3 Å critically dispersed, 20% (73.3 → 58.6%) for 5 Å critically dispersed, and improved to 14% (73.3 → 62.9%) when three times critical dispersion was used with 5 Å bandwidth. The scaled plane wave model predicts 11, 28, and 26% reduction for these measurements, respectively. It is suggested that the better than expected results with bandwidth and SSD are partially a result of local variation of the optic axis direction throughout the volume of the KD*P tripler.

6. ACKNOWLEDGMENT

The authors would like to acknowledge the efforts of F. Penko, E. Padilla, and R. Wilcox to build and test the 17 GHz modulator system. This work was performed under the auspices of the U. S. Department of Energy by Lawrence Livermore National Laboratory under Contract No. W-7405-Eng-48.

7. REFERENCES

1. R. H. Lehmberg and S. P. Obenschain, "Use of induced spatial incoherence for uniform illumination of laser fusion targets," Optics Comm. **46**, 27-31 (1983).

2. Y. Kato, K. Mima, N. Miyanaga, S. Arinaga, Y. Kitagawa, M. Naktsuka, and C. Yamanka, "Random phasing of high-power lasers for uniform target acceleration and plasma instability suppression," Phys. Rev. Lett. **53**, 1057-1060 (1984).
3. R. H. Lehmberg and J. Goldhar, "Use of incoherence to produce smooth and controllable irradiation profiles with KrF fusion lasers," Fusion Technology **11**, 532-541 (1987).
4. D. Véron, H. Ayral, C. Gouedard, D. Husson, J. Lauriou, O. Martin, B. Meyer, M. Rostaing, and C. Sauteret, "Optical spatial smoothing of Nd-glass laser beam," Optics Comm. **65**, 42-45 (1988).
5. S. Skupsky, R. W. Short, T. Kessler, R. S. Craxton, S. Letzring, and J. M. Soures, "Improved laser-beam uniformity using the angular dispersion of frequency-modulated light," J. Appl. Phys. **66**, 3456-3462 (1989).
6. D. Véron, G. Thiell, C. Gouedard, "Optical smoothing of the high power PHEBUS Nd-glass laser using the multimode optical fiber technique," Optics Comm. **97**, 259-271 (1993).
7. R. S. Craxton and S. Skupsky, "2D SSD and polarization wedges for OMEGA and the NIF," Bull. Amer. Phys. Soc. **40**, 1826 (1995); J. E. Rothenberg, "Two dimensional beam smoothing by spectral dispersion for direct drive inertial confinement fusion," Proc. Soc. Photo-Opt. Instrum. Eng. **2633**, pp. 634-644 (1995).
8. D. M. Pennington, M. A. Henesian, S. N. Dixit, H. T. Powell, C. E. Thompson, and T. L. Weiland, "Effect of bandwidth on beam smoothing and frequency conversion at the third harmonic of the Nova laser," Proc. Soc. Photo-Opt. Instrum. Eng. **1870**, 175-185 (1993).
9. J. E. Murray, D. Milam, K. G. Estabrook, and C. D. Boley, "Spatial Filter Issues", in these proceedings.
10. P. J. Wegner, J. M. Auerbach, C. E. Barker, S. C. Burkhart, S. A. Couture, J. J. DeYoreo, R. L. Hibbard, L. W. Liou, M. A. Norton, P. A. Whitman, and L. A. Hackel, "Frequency Converter development for the National Ignition Facility", in these proceedings.
11. D. Eimerl, J. M. Auerbach, C. E. Barker, D. Milam, and P. Milonni, "Multicrystal designs for efficient third-harmonic generation", Optics Lett. **22**, 1208-1210 (1997).